# Structure Conserving Correlation and the Kohlrausch-Williams-Watts Decay of the Incoherent Intermediate Scattering Function in Simulated $Ni_{0.5}Zr_{0.5}$ Melt

H. Teichler

*Institute for Materials Physics, University of Goettingen, 37077 Goettingen, Germany*

(Received 13 September 2010; revised manuscript received 10 February 2011; published 2 August 2011)

Results are presented about the origin of the Kohlrausch-Williams-Watts decay of the incoherent intermediate scattering function (ISF) in molecular dynamics simulated liquid $Ni_{0.5}Zr_{0.5}$. By the concept of weakly effective particles (WEPs), we establish an interrelationship between ISF and particle dynamics. Temporal correlations in the action of WEPs act structure conserving, reflecting that immobile particles tend to remain immobile. Analysis of the related correlation function yields that these correlations account quantitatively for the stretched exponential like decay.

DOI: 10.1103/PhysRevLett.107.067801 PACS numbers: 61.25.Em, 61.20.Ja, 61.20.Lc, 64.70.Q−

The Kohlrausch-Williams-Watts (KWW) decay of fluctuations, often empirically described by the stretched exponential (STX) $\exp\{-(t/\tau)^{\beta}\}$, is observed in various kinds of complex systems such as structural glasses and melts, amorphous polymers, colloidal suspensions, and spin or orientation glasses. Besides its importance by its own as signature of complex systems, KWW decay has gained much interest in the context of glass transition, as this type of relaxation shifts to macroscopic times under cooling, thereby initiating glass formation.

Although rather common in nature, the physics behind the KWW law is a topic under debate. There are highly elaborated and very successful but rather different approaches in this field: Some consider defect mediated relaxation [1–3], which leads to the concept of waiting time distributions. Some emphasize randomness [4], disorder [5] or dynamical heterogeneity, the latter resulting in a broad spectrum of relaxation times [6,7]. Others concentrate on fractal topology of complex systems' configuration space [8,9] or on back-jump effects [10]. Mode coupling theory (MCT) shows that the STX law holds for the $\alpha$-decay of the intermediate scattering function (ISF) in the large-$q$ limit [11]. Moreover, KWW decay is often described by fractal dynamics [12,13].

This list of references is arbitrary and not complete. It indicates, however, the large variety of successful theories in this field. This variety motivated us to analyze molecular dynamics (MD) simulation data for an atomistic picture of the KWW decay in liquids and structural glasses. Our analysis concerns the incoherent ISF of a binary metallic melt. We describe here three aspects of our approach: First, the concept of "strongly" and "weakly effective particles" (SEPs and WEPs), which provides a link between the decay of the ISF and the particle dynamics in the melt; second, the distribution of SEPs in space and time; third, correlations in the time distribution of WEPs, which turn out to give rise to the KWW decay.

Our analysis relies on MD data for a $Ni_{0.5}Zr_{0.5}$ model (see, e.g., [14] and references therein) at nominal 1050 K, just above its glass temperature at the applied cooling rate of $10^9$ K/s. Aimed at simulating a coarse graining volume element, we consider $N_{at} = 648$ particles (324 Ni-, 324 Zr-atoms) in an orthorhombic simulation box with cyclic boundary conditions. After 100 ns isothermal annealing, we record the particle trajectories for 900 ns. Figure 1 shows for Ni and Zr at $q_1 = 21.6\ \mathrm{nm}^{-1}$ the ISF evaluated from $F_\gamma(\tau, \mathbf{q}) = \langle \exp\{i\mathbf{q}\mathbf{u}_n(t, \tau)\}\rangle$ ($\mathbf{u}_n(t, \tau)$: displacement of atom $n$ in time interval $[t, t + \tau]$. The brackets symbolize averaging over $t$ and atoms $n$ of type $\gamma \in \{\mathrm{Ni}, \mathrm{Zr}\}$). Above 0.1 ns the ISFs can be approximated as STX, $\Phi^F_\gamma \exp(-(\tau/\tau^F_\gamma)^{\beta})$, with $\Phi^F_{\mathrm{Ni}} = 0.766$, $\beta^F_{\mathrm{Ni}} = 0.61$, $\tau^F_{\mathrm{Ni}} = 105$ ns for Ni (Zr: $\Phi^F_{\mathrm{Zr}} = 0.826$, $\beta^F_{\mathrm{Zr}} = 0.63$, $\tau^F_{\mathrm{Zr}} = 500$ ns). Definition of $\alpha$ relaxation time $\tau^\gamma_\alpha(q)$ by $F_\gamma(\tau^\gamma_\alpha(q), q) = 1/e$ gives $\tau^{\mathrm{Ni}}_\alpha(q_1) = 63$ ns, $\tau^{\mathrm{Zr}}_\alpha(q_1) = 355$ ns.

The concept of "strongly" and "weakly effective particles" is introduced by recurring to isotropic melts. There, rotation invariance leads to $F_\gamma(\tau, q) = \langle j_0(q u_n(t, \tau))\rangle$, with Bessel function $j_0(z) = \sin(z)/z$. At $\tau = \tau_\alpha{}^\gamma$ the relationship $\langle j_0\rangle = 1/e$ holds. Exploiting that $j_0(z) > 1/e$ for

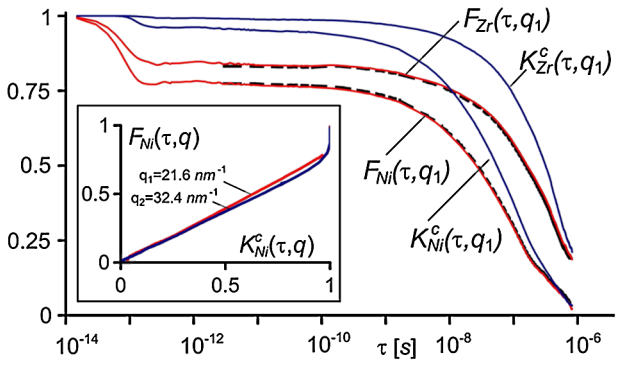


FIG. 1 (color online). ISF $F_\gamma(\tau)$ and fraction of WEPs $K^c_\gamma(\tau)$ for simulated $Ni_{0.5}Zr_{0.5}$ at 1050 K. (dotted lines: ISFs approximated by $\langle j_0\rangle_W K^c_\gamma(\tau)$.)-The inset shows $F_{\mathrm{Ni}}(\tau)$ vs $K^c_{\mathrm{Ni}}(\tau)$ for $q_1$ and $q_2$. (Plots $F_{\mathrm{Zr}}(\tau)$ vs $K^c_{\mathrm{Zr}}(\tau)$ agree with those for Ni within drawing line thickness.)

 © 2011 American Physical Society

$z < z_c \approx 0.7\pi$ and $j_0(z) < 1/e$ for $z > z_c$, we separate the atoms for each $q$ and interval $[t, t+\tau]$ in two classes, "strongly effective particles" with $u_n(t,\tau) > u_c(q) := z_c/q$, and "weakly effective particles" with $u_n(t,\tau) < u_c(q)$. The WEPs keep the value of the ISF above $1/e$. The SEPs tend to reduce it. $q_1 = 21.6\ \mathrm{nm}^{-1}$ means $u_c(q_1) = 0.102$ nm. For the present system, $u_c(q_1) = 0.102$ nm separates in-cage rattling of the particles and out-of-cage escape (cf. [15]).

Figure 1 includes the mean fraction of WEPs

$$K^c_\gamma(\tau, q) = \langle \vartheta_n(t,\tau) \rangle \tag{1}$$

($\vartheta_n(t,\tau) = \Theta\{u_c(q) - u_n(t,\tau)\}$, $\Theta$: Heaviside step function). Like $F_\gamma(\tau, q)$, $K^c_\gamma(\tau, q)$ shows STX-type decay above 0.1 ns (for Ni: $\Phi^K_{\mathrm{Ni}} = 0.953$, $\beta^K_{\mathrm{Ni}}(q_1) = 0.62$, $\tau^K_{\mathrm{Ni}}(q_1) = 110$ ns; for Zr: $\Phi^K_{\mathrm{Zr}} = 0.981$, $\beta^K_{\mathrm{Zr}}(q_1) = 0.69$, $\tau^K_{\mathrm{Zr}}(q_1) = 580$ ns).

In the KWW-region $F_\gamma(\tau)$ and $K^c_\gamma(\tau)$ decrease monotonically with $\tau$. This implies a monotonic increase of $F_\gamma$ as function of $K^c_\gamma$. Then there exists a bijective isomorphism between $K^c_\gamma$ and $F_\gamma$: The former is a unique picture of the latter and vice versa. This allows us to discuss the behavior of $F_\gamma$ in terms of the fraction of WEPs or SEPs and to relate properties of $F_\gamma(\tau, q)$ to atomistic details visible in $K^c_\gamma$.

For quantitative treatment, we introduce the fraction of SEPs by $K_\gamma(\tau, q) = \langle 1 - \vartheta_n(t,\tau) \rangle$ and make use of the decomposition

$$F_\gamma(\tau) = \langle j_0 \rangle_W K^c_\gamma(\tau) + \langle j_0 \rangle_s K_\gamma(\tau). \tag{2}$$

Here $\langle j_0 \rangle_W = \langle j_0(qu_n)\vartheta_n(t,\tau) \rangle / K^c_\gamma(\tau)$ is the mean of $j_0$ over WEPs, $\langle j_0 \rangle_S = \langle j_0(qu_n)(1 - \vartheta_n(t,\tau)) \rangle / K_\gamma(\tau)$ that over SEPs, both depending on $q$, $\tau$, $\gamma$. Regarding Eq. (2), we shall mention two findings from our MD data: First, due to the oscillations of $j_0$ beyond $z_c$, $\langle j_0 \rangle_S K_\gamma$ is a minor contribution to $F_\gamma$ with absolute value smaller than 0.01 and can be neglected in the present context. This is demonstrated in Fig. 1 by the dashed lines, approximating $F_\gamma$ by $\langle j_0 \rangle_W K^c_\gamma(\tau)$. Second, as shown in the inset of Fig. 1, there is a nearly linear relationship between $F_\gamma(\tau, q)$ and $K^c_\gamma(\tau, q)$ in the range of the STX law. According to this, $\langle j_0 \rangle_W$ is nearly independent of $\tau$ and of the fraction of WEPs in the range $0.95 > K^c(\tau) > 0.05$ or $0.05\ \mathrm{ns} < \tau < 500$ ns. Thus, the KWW-decay of $F_\gamma$ reflects the decay of $K^c_\gamma$ with $\tau$, up to minor corrections.

Figure 2 demonstrates the distribution of SEPs in space. For intervals $[t_0, t_0 + \tau]$ with $\tau = 10, 40, 160$ ns, the figure displays the positions $\mathbf{x}_n(t_0)$ of Ni- and Zr-SEPs in the melt, that means of atoms with $u_n(t_0, \tau) > u_c(q_1)$. (All intervals start at time $t_0 = 100$ ns of Fig. 3.) The figures present heterogeneous dynamics with SEPs forming clusters in space, where the increasing cluster size with interval length is in accordance with the results from analyzing

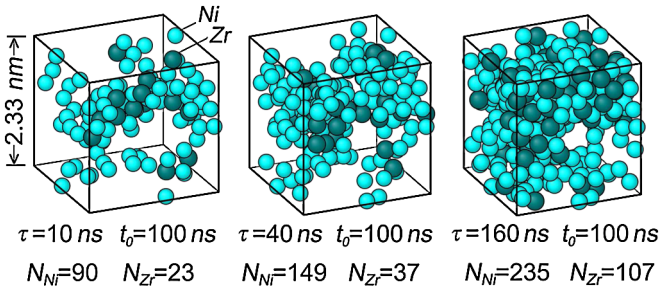


FIG. 2 (color online). Initial position of SEPs in intervals $[t_0, t_0 + \tau]$ for $\tau = 10, 40, 160$ ns. $N_{\mathrm{Ni}}$, $N_{\mathrm{Zr}}$: number of Ni or Zr atoms in the sets of SEPs. (Small spheres: Ni, large spheres: Zr atoms. $t_0 = 100$ ns of Fig. 3.)

dynamic heterogeneity (DH) (see, e.g., the recent review [16] and for the present system [14]).

Figure 3 shows the fraction of Ni-SEPs in intervals $[t_i, t_i + \tau]$ plotted as short horizontal lines against the starting times $t_i$ for various $\tau$. The figure uses equal-spaced $t_i$ with separation 10 ns, covering about 750 ns in total. The $\tau$ values range from 10 to 320 ns and characterize the main part of the $\alpha$ decay in the Ni subsystem from the late-$\beta$ region around 10 ns to the region well beyond $\tau^{\mathrm{Ni}}_\alpha$. The figure displays intermittent dynamics with fluctuating fraction of Ni-SEPs (reflecting the size of the "coarse graining" box). The mean values grow with $\tau$ and agree with $K_{\mathrm{Ni}}(\tau) = 1 - K^c_{\mathrm{Ni}}(\tau)$ from Fig. 1. In Fig. 3, $\Delta^2(\tau)$ is the variance of the fluctuating fraction of SEPs. It corresponds to the self part of the $\chi_4$ susceptibility (in the version of the early DH analysis [17]), up to a factor V/kT (V: volume of simulation box). As function of $\tau$, $\Delta^2$ exhibits the peak structure expected from DH [16,17].

Figure 3 implies that the larger fraction of Ni-SEPs at larger intervals $\tau$ are due to accumulation of low-fraction contributions from short $\tau$. Deviation of the $\alpha$ decay from exponential Debye relaxation relies on correlations during

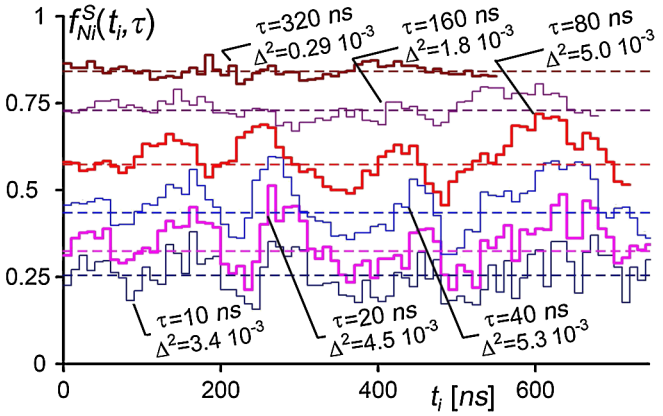


FIG. 3 (color online). Fraction of Ni-SEPs, $f^S_{\mathrm{Ni}}(t_i, \tau)$, in intervals $[t_i, t_i + \tau]$ indicated by short lines vs $t_i = 10i$ ns for $\tau = 10, 20, \ldots 320$ ns. The mean values at fixed $\tau$ agree with $1 - K^c_{Ni}(\tau)$ of Fig. 1. $\Delta^2$: variance of $f^S_{\mathrm{Ni}}(t_i, \tau)$ at fixed $\tau$.

this accumulation. Spatial and temporal correlations of particle dynamics have been successfully studied in the context of DH (see, e.g., [16]) where much emphasize has been laid on searching for a diverging length scale at growing $\tau$. We analyze the correlations by use of the probability $P_W^\gamma(\sigma, \tau)$ for a particle to act as WEP in $[t', t' + \tau]$ when having acted as WEP in the earlier interval $[t, t + \tau]$, with $t' = t + \sigma$,

$$P_W^\gamma(\sigma, \tau) = \langle \vartheta_n(t + \sigma, \tau)\vartheta_n(t, \tau)\rangle / \langle \vartheta_n(t, \tau)\rangle. \quad (3a)$$

We transcribe it as

$$P_W^\gamma(\sigma, \tau) = K_\gamma^c(\tau) + K_\gamma(\tau)\Pi^\gamma(\sigma, \tau), \quad (3b)$$

$$\Pi^\gamma(\sigma, \tau) = \langle \Delta\vartheta_n(t + \sigma, \tau)\Delta\vartheta_n(t, \tau)\rangle / D_0. \quad (4)$$

$\Pi^\gamma(\sigma, \tau)$ measures correlations of fluctuations $\Delta\vartheta_n(t, \tau) = \vartheta_n(t, \tau) - \langle\vartheta_n(\tau)\rangle$. Normalization of $\Pi^\gamma(\sigma, \tau)$ to 1 for $\sigma \to 0$ leads to $D_0 = K_\gamma^c(\tau)K_\gamma(\tau)$. We may introduce the probability of SEPs to remain SEPs in shifted intervals, $P_S^\gamma(\sigma, \tau)$, by changing in Eq. (3a) $\vartheta_n(\ldots, \tau)$ into $1\text{-}\vartheta_n(\ldots, \tau)$. With Eq. (4) then holds $P_S^\gamma(\sigma, \tau) = K_\gamma(\tau) + K_\gamma^c(\tau)\Pi^\gamma(\sigma, \tau)$, which reflects that $\Pi^\gamma(\sigma, \tau)$ measures the correlations in the fluctuations of SEPs, too.

Figure 4 displays $\Pi^{\mathrm{Ni}}(\sigma, \tau)$ for $\tau$-values between 2.5 and 160 ns, plotted against $\sigma/\tau$. For nonoverlapping intervals, $\sigma/\tau > 1$, the finite values of $\Pi^{\mathrm{Ni}}(\sigma, \tau)$ indicate temporal correlations. They make that $P_W^\gamma(\sigma > \tau, \tau)$ is larger than $K_\gamma^c(\tau)$, its value for random transfer between WEPs and SEPs. (This meaning of $K_\gamma^c(\tau)$ follows from Eq. (3a), since there $\vartheta_n(t + \sigma, \tau)$ can be substituted by its average in the random case and $\sigma > \tau$.) Consequently, the relaxation of structure fluctuations is reduced compared to random decay, which means we have "structure conserving correlation" (SCC). SCC can be visualized as temporary partial decomposition of the set of particles in those

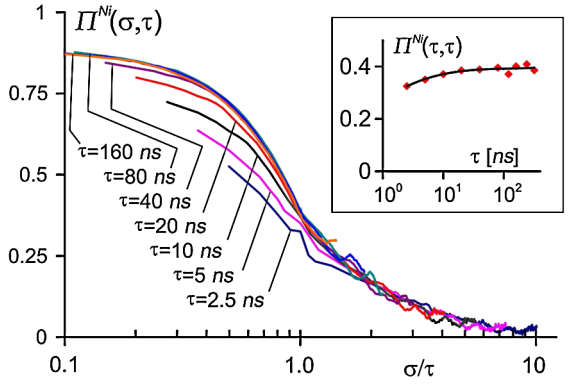


FIG. 4 (color online). Correlation function $\Pi^{\mathrm{Ni}}(\sigma, \tau)$ [see Eq. (4)], characterizing the fraction of Ni-atoms acting as WEPs in $[t + \sigma, t + \sigma + \tau]$ when having acted as WEPs in $[t, t + \tau]$, plotted against $\sigma/\tau$. The inset shows $\Pi^{\mathrm{Ni}}(\tau, \tau)$, the correlation between successive intervals of length $\tau$.

which remain WEPs and those which preferentially act as SEPs for several interval lengths.

SCC plays an important role for the KWW decay of $K_\gamma^c(\tau)$ as the fraction of WEPs in interval $I_0 = [t_i, t_i + 2\tau]$ is determined by the fraction of WEPs in the half-interval $I_1 = [t_i, t_i + \tau]$ and the surviving ones in $[t_i + \tau, t_i + 2\tau]$, modified by minor corrections. There is the (exact) relationship

$$K_\gamma^c(2\tau) = K_\gamma^c(\tau)P_W^\gamma(\tau, \tau) + \delta K_\gamma^c(2\tau) \quad (5)$$

where $\delta K_\gamma^c(2\tau)$ counts particles that act as SEPs in $I_1$ and/or $I_2$ while the combined motion in both half-intervals makes them WEPs in $I_0$, and (with negative sign) those which are WEPs in $I_1$ and $I_2$ while combined displacement makes them SEPs in $I_0$. The latter mean "drifting" particles, the former are back jumping particles, another aspect of SCC.

By Eq. (3b), $K_\gamma^c P_W^\gamma$ in Eq. (5) becomes $K_\gamma^c K_\gamma^c + K_\gamma^c\Pi^\gamma(1 - K_\gamma^c)$. The first term describes hypothetic uncorrelated random transitions of WEPs into SEPs, the second means SCC counteracting this random decay. Including $\delta K_\gamma^c$, there are three terms in Eq. (5) governing the decay of $K_\gamma^c(\tau)$. Understanding the action of these terms allows understanding the atomistic mechanism of KWW-relaxation. Regarding this we present in Fig. 5 iterated solutions of Eq. (5) under various conditions, at left for Ni, right for Zr. Solutions $A$ (dots in Fig. 5) use $\Pi^\gamma(\tau, \tau)$ (given for Ni in the inset of Fig. 4) and $\delta K_\gamma^c(2\tau)$ from the MD data. Solutions $B$ (triangles) rely on constant $\Pi^{*\gamma}$ and $\delta K_\gamma^c = 0$, using $\Pi^{*\mathrm{Ni}} \approx 0.39$ as predicted by the inset of Fig. 4 for Ni in the $\alpha$-decay regime, and $\Pi^{*\mathrm{Zr}} \approx 0.31$ deduced from similar Zr-data. The lines under the symbols are STX-curves. Solutions C (full lines) originate from $\Pi = 0$, $\delta K_\gamma^c = 0$. In this case Eq. (5) predicts exponential Debye decay of $K_\gamma^c$, as the *rhs*. reduces to $(K_\gamma^c)^2$.- In Fig. 5 the $K_\gamma^c(\tau)$ curves are shifted along the $\tau$ axis to coincide at $K^c = 0.925$ in case of Ni ($K^c = 0.975$ in case of Zr).

By construction, solutions A agree with the initial $K_\gamma^c(\tau)$ of Fig. 1, and the STX curves under the dots are those with parameters from the simulated $K_\gamma^c(\tau)$ given below Eq. (1). For solutions B, the STX curves refer to $\Phi^* = 1$ and $\beta_{\mathrm{Ni}}^* = 0.61$, $\beta_{\mathrm{Zr}}^* = 0.71$. Comparing solutions $B$ with $C$ shows that in the $\alpha$-decay regime $\Pi^{*\gamma}$ initiates reduction of $\beta$ from its Debye value 1 to 0.61 for Ni (to 0.71 for Zr). Comparison of solutions $A$ and $B$ indicates that $\delta K_\gamma^c$ has minor effect on $\beta$ but accounts for reduction of the plateau value $\Phi$ and an additional decrease at $\tau > \tau_{\mathrm{Ni}}^K$. The latter is expected from drifting particles at large $\tau$, the former may be ascribed to rapid back-jump processes. The dominant importance of $\Pi^{*\gamma}$ for reducing $\beta$ below 1 is confirmed by a further solution of Eq. (5), not exhibited in Fig. 5, which takes into account $\delta K_\gamma^c(2\tau)$ and the difference $\Pi^\gamma(\tau, \tau) - \Pi^{*\gamma}$, and which shows the reduction of $\Phi$ but yields $\beta_\gamma^* \approx 1$.

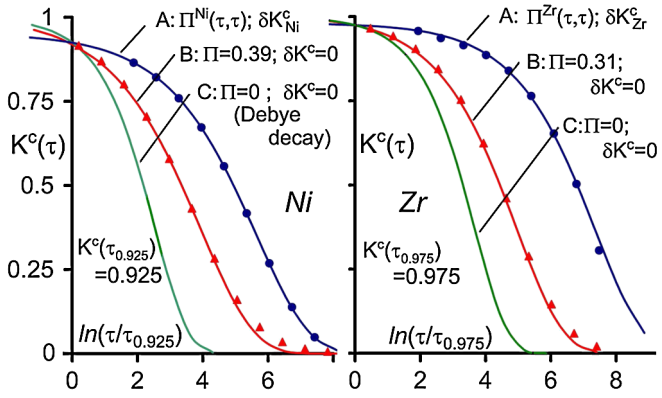


FIG. 5 (color online). Iterated solutions $K_\gamma^c$ of Eq. (5) against $\ln(\tau/\tau_p)$ ($\tau_p$: see text) for Ni (left) and Zr (right). (A) $\Pi_\gamma(\tau,\tau)$, $\delta K_\gamma^c(2\tau)$ from MD data, reproduces the MD curves of Fig. 1; (B) $\Pi^{*\gamma} = 0.39, 0.31$, $\delta K_\gamma^c = 0$ (representative for Ni and Zr in the present model around $\tau_\gamma^K$), yields reasonable stretching parameter $\beta$ but fails regarding plateau value $\Phi$; (C) $\Pi^{*\gamma} = 0$, $\delta K_\gamma^c = 0$, Debye decay. (Full lines: STX-curves; in case C: exponential.)

In case of STX behavior, $\beta$ may be expressed as function of $\Pi^\gamma$ and $\delta K_\gamma^c$ by $\ln(1/\ln\{\Phi_\gamma^K/K_\gamma^c(1/2\tau_\gamma^K)\})/\ln(2)$ with $K_\gamma^c(1/2\tau_\gamma^K)$ from solving Eqs. (5) and (3) for $K_\gamma^c(1/2\tau_\gamma^K)$ at $\tau = 1/2\tau_\gamma^K$, exploiting $K_\gamma^c(\tau_\gamma^K) = \Phi_\gamma^K/e$. In the limit of negligible $\delta K_\gamma^c(\tau_\gamma^K)$ (approximately fulfilled in our MD data by $|\delta K_\gamma^c(\tau_\gamma^K)| < 0.008$ for Ni and Zr) and $\Phi_\gamma^K \to 1$, the resulting $\beta$ values closely follow the relation $\beta \approx 1 - \Pi^\gamma(1/2\tau_\gamma^K)$, with deviation less than 0.01 for $0 < \Pi^\gamma < 1$. This relation gives a quantitative estimate for the interrelation between $\beta$ and $\Pi^\gamma$. It parallels a suggestion by Vogel and Glotzer [18] for a correlation between DH and $\beta$ of the ISF, deduced from analyzing data of various MD models (Silica [18], polymer melt [19(a)], Lennard-Jones mixtures [17,19(b)], water [19(c)], and Djugutov liquid [19(d)]), which show lowest $\beta$ in the Djugutov model with largest DH when measured, for example, by the mean size of clusters of most mobile atoms. Moreover, in the limit of large $q$, MCT predicts $\beta$ independent of $q$ for the ISF [11] and $\beta \to b$, the von-Schweidler exponent of MCT. Thus the here found interrelationship between $\beta$ and $\Pi$ (and eventually $\delta K^c$) implies a connection between the correlation in the survival of WEPs for large $q$ and the MCT exponents.

As discussed in the beginning, due to nearly $\tau$ independent $\langle j_0(q,\tau)\rangle_W$ in the $\alpha$-decay regime, $F_\gamma(\tau,q)$ is a nearly linear function of $K_\gamma^c(\tau,q)$ and reflects the decay of the latter. Thus our analysis unambiguously demonstrates for the present example that the KWW decay of $F_\gamma(\tau,q_1)$ is due to temporal correlations in the survival of WEPs, initiating non-Markovian dynamics. (Similar conclusions can be drawn for the ISFs at $q_2$.) Sources of such correlations are, for example, the phenomena considered in the context of spatial DH (e.g., [16–19]) ranging from structure related heterogeneity in the sense of propensity [20] to dynamics initiated in the genuine sense of dynamical facilitation [21]. However, one should have in mind that temporal dynamic correlations may exist without spatial DH (e.g., [4]), and that correlations in terms of preferred back jumps [10] may be an alternative, although being negligible for characterizing the origin of KWW-decay here. Our results imply that rather different physical phenomena can lead to KWW-type decay, provided they yield suitable correlations or atomic trajectories reflecting such correlations. This may explain the success of the broad spectrum of theories in this field addressed in the introduction.

[1] M. F. Shlesinger and E. W. Montroll, Proc. Natl. Acad. Sci. U.S.A. **81**, 1280 (1984).
[2] J. T. Bendler and M. F. Shlesinger, J. Mol. Liq. **36**, 37 (1987); J. T. Bendler and M. F. Shlesinger, Macromolecules **18**, 591 (1985).
[3] J. Klafter and M. F. Shlesinger, Proc. Natl. Acad. Sci. U.S.A. **83**, 848 (1986).
[4] B. Sturman, E. Podivilov, and M. Gorkunov, Phys. Rev. Lett. **91**, 176602 (2003).
[5] F. Sciortino and P. Tartaglia, Physica A (Amsterdam) **236**, 140 (1997).
[6] R. V. Chamberlin, Phys. Rev. Lett. **82**, 2520 (1999).
[7] X. Xia and P. G. Wolynes, Phys. Rev. Lett. **86**, 5526 (2001).
[8] P. Jund, R. Jullien, and I. Campbell, Phys. Rev. B **63**, 036131 (2001).
[9] J. R. Macdonald and J. C. Phillips, J. Chem. Phys. **122**, 074510 (2005).
[10] K. Funke and R. Hoppe, Solid State Ionics **40–41**, 200 (1990).
[11] M. Fuchs, J. Non-Cryst. Solids **172–174**, 241 (1994).
[12] R. Metzler and J. Klafter, Phys. Rep. **339**, 1 (2000).
[13] A. Jurlewicz and K. Weron, J. Non-Cryst. Solids **305**, 112 (2002).
[14] I. Ladadwa and H. Teichler, Phys. Rev. E **73**, 031501 (2006); I. Ladadwa and H. Teichler, Phys. Rev. E **78**, 041503 (2008).
[15] H. Teichler, Phys. Rev. E **71**, 031505 (2005).
[16] L. Berthier, G. Biroli, J.-B. Bouchaud, and R. L. Jack, arXiv:1009.4765.
[17] N. Lacevic, F. W. Starr, T. B. Schroder, and S. C. Glotzer, J. Chem. Phys. **119**, 7372 (2003).
[18] M. Vogel and S. C. Glotzer, Phys. Rev. E **70**, 061504 (2004).
[19] (a) M. Aichele, Y. Gebremichael, F. W. Starr, J. Baschnagel, and S. C. Glotzer, J. Chem. Phys. **119**, 5290 (2003); (b) C. Donati, S. C. Glotzer, P. H. Poole, W. Kob, and S. J. Plimpton, Phys. Rev. E **60**, 3107 (1999); (c) N. Giovambattisit, S. V. Buldyrev, F. W. Starr, and H. E. Stanley, Phys. Rev. Lett. **90**, 085506 (2003); (d) Y. Gebremichael, M. Vogel, and S. C. Glotzer, J. Chem. Phys. **120**, 4415 (2004).
[20] A. Widmer-Cooper, P. Harrowell, and H. Fynewever, Phys. Rev. Lett. **93**, 135701 (2004).
[21] J. P. Garrahan and D. Chandler, Phys. Rev. Lett. **89**, 035704 (2002); D. Chandler and J. D. Garrahan, J. Chem. Phys. **123**, 044511 (2005).